RSC Advances

PAPER

View Article Online
View Journal | View Issue

Cite this: *RSC Adv.*, 2020, **10**, 35341

Ag@TiO_2NPs/PU composite fabric with special wettability for separating various water–oil emulsions†

Ming Zhang,[a] Daxin Liang,[b] Wei Jiang*[c] and Junyou Shi*[a]

Received 18th July 2020
Accepted 10th September 2020

DOI: 10.1039/d0ra06248k

rsc.li/rsc-advances

In the present study, Ag@TiO_2 nanoparticles (NPs) were successfully synthesized by a hydrothermal method. Then the fabric (treated by dielectric barrier discharge (DBD) plasma and alkali desizing) was sprayed by solutions of polyurethane (PU) adhesive and as-prepared Ag@TiO_2NPs in sequence for constructing a robust multi-level structure. Afterwards, the durable superhydrophilic and underwater superoleophobic coatings were obtained on the fabric surface. With further octadecyl trichlorosilane (OTS) modification, the wetting behaviour of the coating was transferred to superhydrophobicity and superoleophilicity. Observations showed that both cotton fabrics exhibited excellent superwetting properties and antimicrobial activities even after experiencing repeated rinsing by water or oil, abrasion with the original cotton fabric or sand paper, and in chemical stability tests in a base and acid, *etc.* Moreover, the two types of Ag@TiO_2NPs/PU composite fabrics could successfully serve as filtering membranes for the fine reclamation of water or oil from their emulsion mixtures, which demonstrated high selectivity and efficiency, offering the theoretical foundation to extend the range of practical applications for textiles.

Introduction

The oil pollution derived from oil spill accidents and the improper effluent discharge from petrochemical, textile and food industries lead to great loss of energy resources and long-term damaging effects on the ecological environment.[1–3] Generally, oil/water mixtures are composed of an immiscible mixture and emulsified mixture. The conventional methods (*e.g.* ultrasonic separation, flotation and skimming) to separate a liquid mixture have many limitations, such as a low separation efficiency, high energy cost and secondary pollution.[4–6] Besides, they are not applicable to separate oil/water emulsions (*e.g.* oil-in-water and water-in-oil emulsions by formulation, surfactant-stabilized and surfactant-free emulsions by their components),[7,8] which prefer remaining in multiple states. Materials with a selective superwetting property towards water or oil could be primely utilized to separate or even purify oil contamination.[9,10]

Fibrous materials that are multi-porous with a high surface-to-volume ratio and selective superwetting properties towards water or oil are the most desired products for water/oil separation. Nowadays, the existing technologies for endowing fibrous substrates with special wetting properties include chemical deposition,[11] radiation-induced graft polymerization,[12] lithographic patterning,[13] phase separation,[14] sol–gel processing,[15] electrospinning,[7,8] the self-assembly of block copolymers,[16] layer-by-layer self-assembly (LBL)[17] and hyperbaric spraying.[18,19] For instance, Wang *et al.* reported a Janus fabric membrane with opposite superwetting properties, which could serve as a filter for separating oil from oil-in-water emulsions efficiently and directionally.[20] Yang *et al.* further explored the current and potential applications of the Janus membrane in the directional transport, switchable permeation and performance optimization with detailed mechanisms.[21] As is well known, most materials with special wetting properties have limitations for practical use because of the multi-step procedures for implementation, poor durability in harsh conditions, limitations in substrate size, *etc.* Therefore, it is a research hotspot to research and develop a facile and simple method to obtain materials with robust superwetting properties.

PU is popular for its elasticity and has been widely applied in the textile industry in recent years for manufacturing various elastic yarns and fabrics.[22] Meanwhile, PU adhesive possesses superior tackiness with substrates containing hydrogen, *e.g.* foam, plastic, wood, leather, fabric, paper, ceramics and other

[a]Jilin Provincial Key Laboratory of Wooden Materials Science and Engineering, Beihua University, Jilin 132013, China. E-mail: mattzhming@163.com; junyoushi468@163.com

[b]Key Laboratory of Bio-based Material Science and Technology, Ministry of Education, Northeast Forestry University, Harbin 150040, China. E-mail: daxin.liang@nefu.edu.cn

[c]State Key Laboratory of Bio-Fibers and Eco-Textiles, Qingdao University, Qingdao 266000, China. E-mail: weijiangqd@qdu.edu.cn

† Electronic supplementary information (ESI) available. See DOI: 10.1039/d0ra06248k

porous materials.[23] Both Ag and TiO_2 have effective and broad antibacterial activities, and they are quite friendly towards humans.[24,25] Thus, Ag@TiO_2 NP is a promising material for applying around the house, hospital and living things. Cotton fabric is an active and tailored material with abundant hydroxyl groups, a flexible property, low price and density, good mechanical stability and biodegradability, which enable it to be used in many places. Herein, we tried to endow the cotton fabric with a superwetting property and antimicrobial activity at the same time for expanding the application areas of textile products. Specifically, PU and as-obtained Ag@TiO_2 NPs were assembled onto fabric samples in sequence by a simple spraying method, some of which were further modified with octadecyl trichlorosilane (OTS). Then two types of robust superwetting (*e.g.* superhydrophilic and underwater superoleophobic, superhydrophobic and superoleophilic) fibrous membrane were achieved. The results showed that both fabric products indeed exhibited excellent performances in separating various oil/water emulsion mixtures and resisting different bacteria.

Experimental

Tetrabutyl orthotitanate (TBOT, 98.0%), ethanol (99.7%), diethanol amine (99.0%), sodium hydroxide (96.0%) and trisodium citrate dihydrate (99.0%) were purchased from Tianjin Yongda Chemical Reagent Co., Ltd. Acetone, *n*-hexane, chloroform, 1,2-dichloroethane, Span-80, Tween-80 and one-component PU adhesive were purchased from Tianjin Damao Chemical Reagent Factory. Silver nitrate (99.8%) and OTS were purchased from Tianjin Fuyu Fine Chemical Co., Ltd and Shanghai Macklin Biochemical Co., Ltd, respectively. All the reagents were used as received without further purification. Fabric (100% cotton) was obtained locally, which was treated with DBD plasma (Nanjing Suman Plasma Technology Co., Ltd), desized in NaOH solution (5.0 g L^{-1}) for 10 min, and dried in an oven at 80 °C.

TBOT, ethanol, diethanol amine and de-ionized water were mixed under stirring, and then transferred to a Teflon-lined reactor, which was further placed in an oven heated from room temperature to 140 °C for 6 h. Afterwards, the TiO_2 NPs was unloaded, collected, cleaned and dried in a vacuum oven at 45 °C. Then the TiO_2 NPs (0.2 g), $AgNO_3$ (2.0 g) and $Na_3C_6H_5O_7$ (0.64 g) were dispersed or dissolved into a mixture of de-ionized water (25 mL) and ethanol (25 mL) under stirring for 3 h, and the collected NPs was heated in nitrogen atmosphere from 20 °C to 500 °C at a heating rate of 5 °C min^{-1} for 3 h. Finally, the Ag@TiO_2 NPs were obtained. PU adhesive solution (1.0 wt%, acetone) and Ag@TiO_2 suspension (0.25 g mL^{-1}, ethanol) were prepared and sprayed onto the fabric sample orderly by a spraying gun (the nozzle diameter: 0.5 mm) with 70 psi air pressure. The interval was 6 h, and the dried fabric sample was called "S1". Then S1 turned to "S2" after immersing in the OTS solution (1%, v/v in *n*-hexane) and drying in a vacuum oven at 60 °C. Finally, the superwetting fabric membranes (S1 and S2) were obtained.

The morphologies of the samples were characterized by field emission-environment scanning electron microscopy (FE-ESEM, Quanta FEG 250). The elemental compositions of the samples were determined by an energy dispersive spectrometry (EDS) system, which was connected with the FE-ESEM. The size distributions of the samples were measured by a particle size analyzer (Microtrac, Wave II) in deionized water. The compositions of the coatings assembled on S1 or S2 were analyzed by Fourier transform infrared spectroscopy (FTIR, Magna-IR 560). The wetting properties of the sample were evaluated by a contact angle measuring instrument (Powreach, JC2000C), and the final contact angle (CA) was determined by averaging measurements taken from at least five positions on each sample. The antimicrobial activities of the samples against *Escherichia coli* and *Staphylococcus aureus* were evaluated by the bacterial inhibition ring method. Specifically, beef extract peptone was cast onto empty Petri plates, which were then autoclaved and cooled. Then the bacterium solution with a dilution degree of 10^{-4} was inoculated, and the fabric sample was planted onto the peptone plate, which was further incubated at 37 °C for 24 h.

Results and discussion

As seen in Fig. 1 and S1 (ESI),† the TiO_2 NPs showed a spherical shape and a good mono dispersity with an average diameter of approximately 157 nm, while the Ag@TiO_2 NPs size concentrated in 1.143 μm (72.1%) and 332 nm (27.9%) turned out to be larger and irregular. This was because the presence of Ag NPs loading onto the TiO_2 led to the serious agglomeration of the Ag@TiO_2 NPs. Fig. 1d presents the XRD patterns of TiO_2 NPs and Ag@TiO_2 NPs. The diffraction peaks at 25.3°, 37.9°, 47.9°, 54.5°, 62.6°, 69.1° and 75.2° belonged to the (101), (004), (200), (211), (204), (116) and (215) crystal planes of anatase TiO_2 (JCPDS file no. 21-1272). New diffraction peaks of Ag@TiO_2 XRD

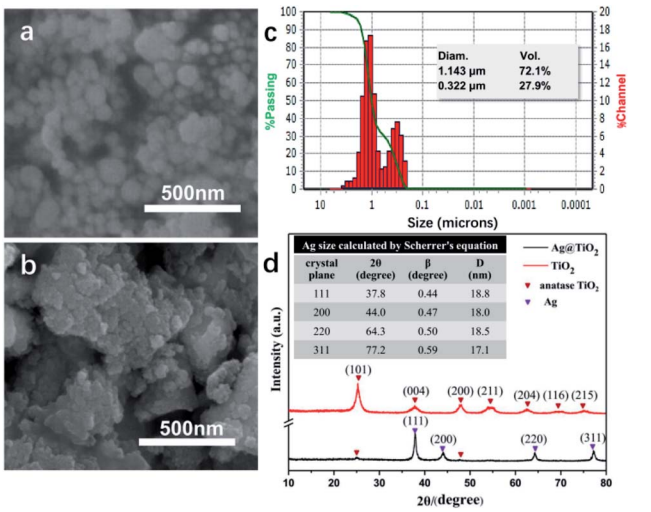

Fig. 1 SEM images of (a) TiO_2 NPs and (b) Ag@TiO_2 NPs. (c) Size distribution of Ag@TiO_2 NPs in deionized water. (d) XRD patterns of TiO_2 NPs and Ag@TiO_2 NPs.

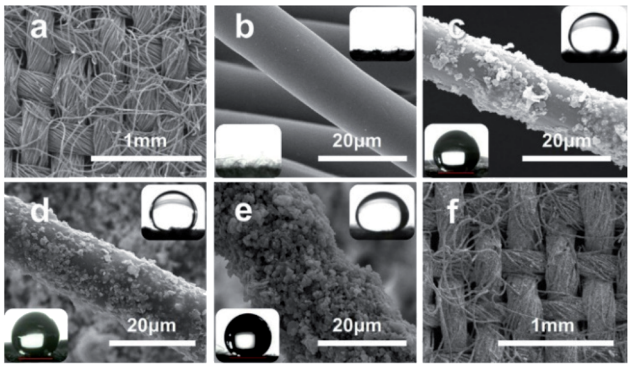

Fig. 2 SEM images: (a) original fabric; (b) plasma and alkali-treated fabric fibre; Ag@TiO_2/PU composite fibre sprayed (c) once, (d) three and (e) five times; (f) Ag@TiO_2/PU composite fabric. Inserts in (b–e) OCA underwater images (upper right) of the plasma and alkali-treated fabric samples, S1-1, S1-3 and S1-5; WCA in air images (lower left) of the plasma and alkali-treated fabric samples, S2-1, S2-3 and S2-5.

pattern appeared at 37.8°, 44.0°, 64.3° and 77.2°, which corresponded to the (111), (200), (220) and (311) planes for the face centred cubic phase of Ag (JCPDS file no. 04-0783). However, we hardly found any diffraction peaks of TiO_2 in Fig. 1d, which was attributed to the wrapping effect of Ag NPs onto the TiO_2 sphere surface. The average size of the Ag NPs could be calculated by Scherrer's equation (eqn (1)):

$$D = \frac{0.89\lambda}{B\cos\theta} \quad (1)$$

where D is the average crystallite domain size perpendicular to the reflecting planes, λ is the X-ray wavelength, β is the full width at half maximum (FWHM), and θ is the diffraction angle. Here, the X-ray wavelength was 0.154056 nm, while β (°) should be transformed to B (radian). The data are listed in the table from the XRD pattern, which was inserted in Fig. 1d. Apparently, the average size of Ag NPs on the TiO_2 sphere surface was 18.1 nm.

The original cotton fabric was composed of numerous cotton fibres at the micrometre level (with an average diameter of 15 μm), which were woven neatly and orderly (Fig. 2a). As seen in Fig. 2b and its inserts, the fibres after DBD plasma and alkali desizing treatments were quite smooth and superlyophilic. After spraying PU solution and Ag@TiO_2 suspension in sequence, numerous granules were caught and adhered onto the PU layer on the fibre surface (Fig. 2c). With the increasing spraying circles, more and more NPs emerged and roughened the substrate. However, the excess Ag@TiO_2 NPs led to the agglomeration and slippage of the coating on the cotton fibre, as shown in Fig. 2c–e. The images of 1,2-dichloroethane droplets dipping onto S1 underwater (upper right) and water droplets dipping onto S2 (left lower) have been inserted in Fig. 2c–e. From the inserts and Table 1, we found that S1 and S2 after suffering three spraying treatments (S1-3 and S2-3) exhibited the best superwetting performance, *e.g.* S1-3 with a water contact angle (WCA) of 6.5° in air and an oil contact angle (OCA) of 159.5° underwater (see Fig. 2d upper right), S2-3 with a WCA of 156.5° in air (see Fig. 2d left lower) and OCA of 0° in air. Significantly, the as-obtained Ag@TiO_2/PU composite fabric still kept its network pores and woven structure, which would be beneficial to fluid transportation and filtration. Therefore, S1-3 and S2-3 became the optimal selections in this research for further separating and purifying experiments towards oil-in-water and water-in-oil emulsions.

The dynamic contact angles (*e.g.* sliding angle (SA)) of the above samples were further investigated for verifying their superwetting properties, *e.g.* S1-3 with the OSA of 6° underwater, S2-3 with the WSA of 8° in air. Meanwhile, we also

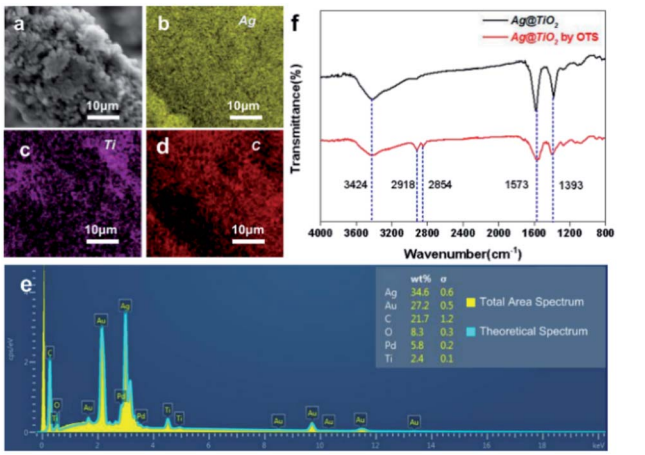

Fig. 3 (a) SEM image of Ag@TiO_2/PU composite cotton fibre; (b) silver, (c) titanium and (d) carbon elemental distributions by EDX; (e) EDX spectrum of the Ag@TiO_2/PU composite cotton fibre; (f) FT-IR spectra of Ag@TiO_2 coating before and after OTS modification.

Table 1 Wetting behaviour and CA of cotton fabric samples before and after treatment

		Before OTS modification		After OTS modification	
Sample name		WCA in air (°)	OCA underwater (°)	WCA in air (°)	OCA in air (°)
Alkali-treated fabric		0	139	147	0
PU coated fabric		133.5	140	—	—
Fabrics with different spraying circles	1	67	151	150	0
	3	6.5	159.5	156.5	0
	5	0	149	154	0

Table 2 Calculated data according to the Wenzel equation and Cassie–Baxter equation

		Wenzel model			Cassie model			
Sample name		θ_w	θ	r	θ_c	θ	f_s (%)	$1 - f_s$ (%)
Smooth OTS film		—	106	—	—	106	—	—
OTS modified fabric		147	—	3.04	147	—	22.27	77.73
Fabrics with different spraying circles	1	150	—	3.14	150	—	18.50	81.50
	3	156.5	—	3.33	156.5	—	11.45	88.55
	5	154	—	3.26	154	—	13.97	86.03

investigated how the roughness and microstructure influenced the wetting properties of samples. The roughness of the fabric before and after spraying Ag@TiO_2/PU was analyzed according to the Wenzel equation (eqn (2)) and Cassie–Baxter equation (eqn (3)):

$$\cos\theta_w = r\frac{\gamma_{sg} - \gamma_{sl}}{\gamma_{lg}} = r\cos\theta \quad (2)$$

$$\cos\theta_c = f_s(\cos\theta + 1) - 1 \quad (3)$$

where θ_w (or θ_c) and θ are the WCAs on the rough and smooth surfaces, respectively, and r is the roughness factor, defined as the ratio of the actual surface area of the rough surface to the geometric projected area, which is always larger than 1. Additionally, f_s and $1 - f_s$ are the fractions of solid contact area and air contact area with water, respectively. Table 2 shows the calculated data through eqn (2) and (3) based on the WCAs of the OTS-modified fabric samples before and after spraying different layers of Ag@TiO_2/PU. Specifically, the roughness factor and fraction of air in contact with water of the OTS-modified fabric after spraying Ag@TiO_2/PU for three circles (S2-3) were the largest, which were 3.33 and 88.55%, respectively. In comparison, the roughness factor and fraction of air in contact with water for the OTS-modified fabric without coating Ag@TiO_2/PU were 3.04 and 77.73%, respectively. Indicating apparently, much more air was trapped in S2-3 under the water droplet. This firmly demonstrated that Ag@TiO_2/PU indeed increased the roughness of the fabric substrate largely, which was the key issue to control the wetting behaviour of the fabric. Furthermore, the WCA of the PU-coated fabric was 133.5°, which was much lower than the OTS-modified one (147°), indicating the significance of selecting materials with the appropriate surface energy as well.

The elemental distribution of a random fibre from S1 (yellow-silver-Ag, violet-titanium-TiO_2, red-carbon-cotton/resin) fully identified the perfect assemblies of Ag NPs on the TiO_2 and Ag@TiO_2/PU composite on the fibre (Fig. 3a–d). In addition, the energy disperse spectrum of S1 is provided in Fig. 3e, displaying its elemental composition of Ag/C/O/Ti (34.6/21.7/8.3/2.4). The reasons for the absence of N element in the EDX spectrum were as follows: (1) the content of N element in PU was not abundant, (2) the layer of PU, offering the bonding effect, located between the fabric and the Ag@TiO_2NPs, and (3) after further spraying with Au, the N element would be totally covered. Meanwhile, the FTIR spectra of Ag@TiO_2 NPs before and after hydrophobic modification in the range of 4000–800 cm^{-1} are presented in Fig. 3f. Specifically, absorption peaks at 3424 and 1573 cm^{-1} in both spectra were respectively attributed to the O–H stretching and bending vibrations, which resulted from the abundant hydroxyl groups on the TiO_2 surface.[26] In comparison, two new absorption peaks around 2854 and 2918 cm^{-1} appeared in the spectrum of the modified Ag@TiO_2, which stemmed from $-CH_3$ and $-CH_2$ asymmetrical and symmetrical stretching vibrations, respectively. This indicated the successful decoration of the long-chain alkyl group (OTS) onto the Ag@TiO_2 NPs.[27]

Oil-in-water and water-in-oil emulsions were prepared as follows:[28] (1) 0.32 g Tween-80, 2 mL chloroform and 120 mL water were mixed and stirred for 3 h (Fig. 4a, chloroform droplet diameter: 4–110 nm); (2) 0.5 g Span-80, 1 mL water and 114 mL chloroform were mixed and stirred for 3 h (Fig. 4b, water droplet diameter: 0.5–10 μm). For separating the emulsions, the common operation involved pouring the mixtures onto S1-3 (or S2-3) as presented in Fig. 4. Specifically, when the chloroform-in-water (C/W) emulsion was poured onto S1-3, the water immediately permeated through the fabric, while the chloroform was only retained on the top of S1-3 till it was transferred to other containers for further measurement. After careful evaluation and calculation, the separation efficiency and flux of S1-3 towards the C/W emulsion were 98.99% and 924.16 L m^{-2}

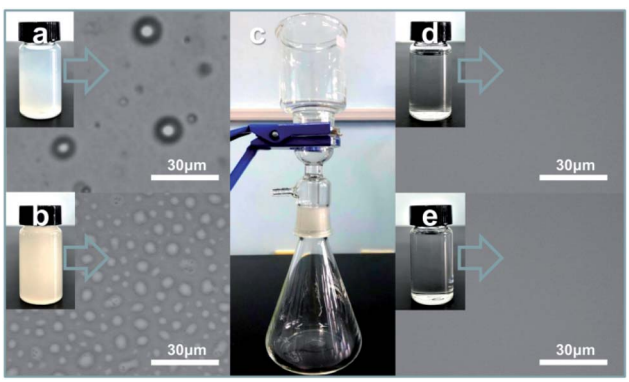

Fig. 4 Photographs and corresponding optical images of (a) C/W and (b) W/C emulsions before filtration; (c) picture of the separating device with S1-3 and S2-3 for the filtration procedure; photographs and corresponding optical images of the filtrates from (d) C/W and (e) W/C emulsions.

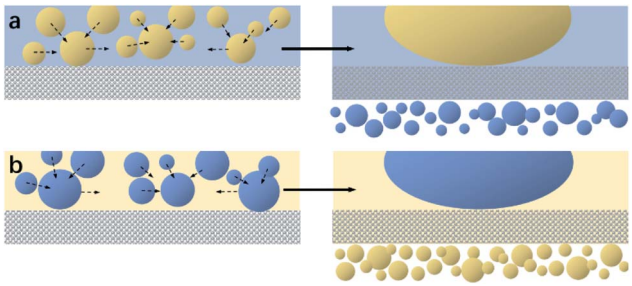

Fig. 5 Separating mechanisms diagrams of (a) S1-3 towards an oil-in-water emulsion and (b) S2-3 towards a water-in-oil emulsion.

h^{-1}, respectively. Then the filtrate was examined by an optical microscope, also displaying an excellent separating effect (Fig. 4d). Meanwhile, when the water-in-chloroform (W/C) emulsion was poured onto S2-3, the water was retained on the top of S2-3, while the chloroform freely permeated through S2-3. The separation efficiency and flux of S2-3 towards the W/C emulsion were 97.98% and 1341.72 L m^{-2} h^{-1}, respectively. Fig. 4e exhibits the optical image of the filtrate after separation, further verifying the remarkable processing effect. Notably, the chloroform (water) could be removed efficiently even though the filtration was repeated 60 times, fully testifying the outstanding performance and endurance of our products (S1-3 and S2-3) for water/oil emulsion separation.

The mechanisms for separating water/oil emulsions throughout S1-3 and S2-3 are presented in Fig. 5. During the separating procedure towards the oil-in-water emulsion (or water-in-oil emulsion) by S1-3 (or S2-3), the water (or oil) would wet and penetrate the sample immediately, as shown in Fig. 5a or b, while the micron oil (or water) droplets in the water (or oil) phase would be rejected by the fabric sample, which would deform, move and further coalesce into the larger oil (or water) droplets standing on the top of membrane for completing the demulsification procedure. Afterwards, these larger oil (or water) droplets could be easily detached from the surface of S1-3 (or S2-3) by a simple rinsing treatment. Finally, the oil contaminants were removed away (or collected) from their emulsion mixtures.

As shown in Fig. 6, the Ag@TiO_2/PU composite fabric (S1-1, S1-3 or S1-5, D: 7.50 mm) could kill all the bacteria (*E. coli* and *S. aureus*) surrounding, which displayed an outstanding antibacterial activity. From Fig. 6g, S1-3 exhibited the best, *e.g.* antibacterial ring thicknesses were 1.81 mm against *E. coli* and 18.82 mm against *S. aureus*. The antibacterial mechanism comprised two parts. First of all, the electronic structure of TiO_2 consisted of a full valence band and an empty conducting band, leading to the photocatalytic performance as follows:[29]

$$TiO_2 + h\nu = h^+ + e^- \rightarrow H_2O + h^+ = HO^\bullet + H^+$$

$$O_2^\bullet + H^+ + e^- = HO_2^\bullet \rightarrow HO_2^\bullet + e^- = HO_2^- \rightarrow HO_2^- + H^+ = H_2O_2$$

$$H_2O_2 + O_2^- = HO^\bullet + OH^- + O_2 \rightarrow H_2O_2 + e^- = HO^\bullet + OH^- \rightarrow OH^- + h^+ = HO^\bullet$$

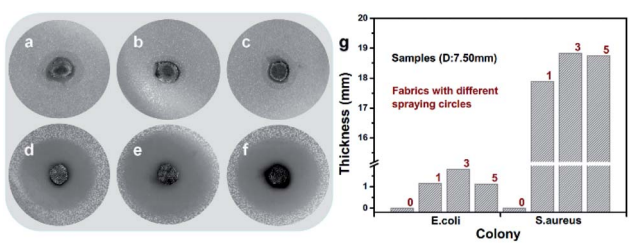

Fig. 6 Photographs of S1-1, S1-3 and S1-5 placed on the peptone plate inoculated with (a–c) *E. coli* and (d–f) *S. aureus*; (g) ring thickness of the original fabric, S1-1, S1-3 and S1-5 placed on the peptone plate inoculated with *E. coli* and *S. aureus*.

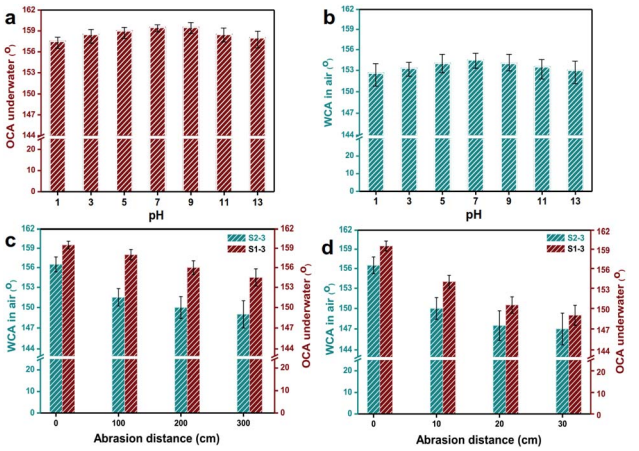

Fig. 7 Relationships between the wetting behaviour and pH of immersing water for (a) S1-3 and (b) S2-3. Correlations between the wetting behaviour and abrasion distance by (c) the cotton fabric and (d) sand paper for S1-3 and S2-3.

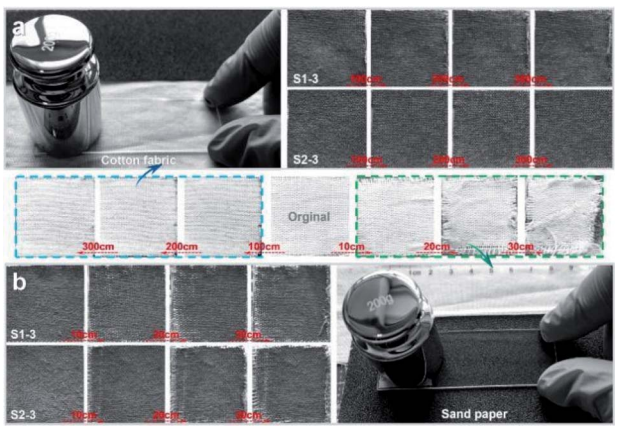

Fig. 8 Photographs of S1-3 and S2-3 after the abrasion tests with (a) cotton fabric and (b) sand paper. Images between Fig. 7a and b show the original fabric before and after the abrasion tests with cotton fabric and sand paper. Loading weight was 200 g, and the abrasion distance is signed in the above images.

Table 3 Separation efficiencies of S1-3 and S2-3 towards C/W and W/C emulsions after repeated rinsing by water or oil, chemical stability test in acid and base, and abrasion with original cotton fabric or sand paper

		Separation efficiency towards C/W and W/C emulsions (%)					
		Rinsing test		Immersing test		Abrasion test	
Sample name		$Water_{60}$	Oil_{60}	pH = 1	pH = 13	$Fabric_{300}$	$Sand\ paper_{30}$
S1-3	C/W	98.76	98.87	97.14	98.69	96.60	95.32
S2-3	W/C	97.63	96.75	96.98	97.49	93.81	92.93

The generated HO$^{\bullet}$ and H_2O_2 aggravated the bacterial decomposition. However, the TiO_2 only absorbed the light with excitation wavelength under 385 nm, while the Ag adhered to TiO_2 (Ag@TiO_2) could make up this shortage in this work. Specifically, the Ag NPs could combine with the hydrosulphonyl in zymoprotein from bacteria tightly to cause the protein to coagulate, and to destroy the cellular synthase activity of the bacteria to deprive its proliferation and development. Moreover, the dissolving Ag^+ would further combine with the membrane protein of bacteria leading to the leakage of matter from within the membrane, thus interfering with the synthesis of peptidoglycan blocking the cell wall synthesis, and effectively preventing the growth of *E. coli*, *S. aureus* and other bacteria or fungus.[24] Most importantly, the Ag^+ would dissociate from the inactivated thallus, and continue its bactericidal activities.

For practical usage, various durable evaluations, including repeating rinsing, immersing in base/acid, periodic abrasion, were applied to S1-3 and S2-3. To be specific, there were no visible changes appearing to S1-3 and S2-3 after rinsing-drying-rinsing circles for sixty times by water, methanol, ethanol, *n*-hexane, gasoline or chloroform. After immersing in the aqueous solution with a pH of 1 and 13 over 20 min, the OCA underwater of S1-3 was always above 157.5° (Fig. 7a), and the WCA in air of S2-3 declined slightly but stayed above 152.5° (Fig. 7b). Meanwhile, there were no visible changes happening to the WCA in air for S1-3 and the OCA in air for S2-3.

Fig. 8 presents the statuses of S1-3 and S2-3 after abrasion tests by cotton fabric and sand paper with a loading weight of 200 g. With the increasing abrasion distance, the Ag@TiO_2/PU coatings on fabrics surface were damaged gradually (Fig. 8a), especially the samples rubbed by sand paper (Fig. 8b). In comparison, the original fabric almost collapsed after rubbing by sand paper with a distance of 30 cm, while our S1-3 and S2-3 performed pretty well. Notably, the OCA underwater of S1-3 and WCA in air of S2-3 after abrasion (with the original cotton textile or sand paper) decreased along with the increasing abrasion distance, and the degrading tendency of both samples with sand paper was quicker than the ones with cotton textile. However, the degrading tendencies of both samples turned to slower along with the increasing abrasion distance. As seen in Fig. 7c and Table S1,† the OCA underwater of S1-3 and WCA in air of S2-3 after rubbing for 300 cm by the original cotton fabric were reduced to 154.5° and 149°, respectively, while their WCA and OCA in air were always 0°. When S1-3 and S2-3 were rubbed by sand paper with a distance of 30 cm, their OCA underwater and WCA in air after rubbing were reduced to 149° and 147° (Fig. 7d), while their OCAs in air were always 0°. In addition, the CA and SA of S1-3 and S2-3 after repeated rinsing by water or oil, and after the chemical stability test in acid and base, and after abrasion with original cotton fabric or sand paper are also presented in Table S1 (ESI)† for further purifying their superwetting durability. These observations not only indicated the as-obtained Ag@TiO_2/PU coatings could prevent the fabric from daily wear and tear, but also demonstrated the remarkable adhesive property between the fabric fibre and Ag@TiO_2/PU coating.

Moreover, the separation efficiencies of S1-3 and S2-3 towards C/W and W/C emulsions after the above-mentioned evaluations were also investigated carefully. From Table 3, we found their efficiencies were all decreased, especially when S1-3 and S2-3 experienced the abrasion test by sand paper. However, the separation efficiencies were always greater than 95% for S1-3 towards the C/W emulsion, and larger than 92% for S2-3 towards the W/C emulsion all the time. Apparently, the results demonstrated that: (1) the Ag@TiO_2/PU coating was tightly adhered to the cotton fibre after the spraying process; (2) OTS was successfully and firmly grafted onto the coating during hydrophobic modification; (3) S1-3 and S2-3 were strong enough to overcome repeated abrasion, immersing and rinsing tests, and always kept their excellent superwetting property and outstanding separating efficiency, which qualifies them for practical fine separations towards oil-in-water and water-in-oil emulsions.

Conclusions

As a summary, Ag NPs were successfully loaded onto TiO_2 NPs for achieving Ag@TiO_2 NPs, which was the key for building robust binary roughness on a fabric substrate. To strengthen the interface between the functional film and substrate and to overcome the weakness (*e.g.* poor durability) of most superwetting materials, we pretreated the substrate with DBD plasma and alkali desizing, and introduced PU adhesive in a simple spraying method. Then a long-lasting superhydrophilic and underwater superoleophobic cotton fabric product (S1-3) was obtained. After further OTS modification, a durable superhydrophobic and superoleophilic cotton fabric product (S2-3) was achieved as well. The results showed that S1-2 and S2-3 always offered an excellent superwetting property even after experiencing repeated rinsing by water or oil, abrasion with

original cotton fabric or sand paper, and chemical stability tests in a base and acid. Moreover, they displayed outstanding antimicrobial activity, which could effectively kill *E. coli* and *S. aureus*. Significantly, S1-2 and S2-3 were successfully applied to the fine filtration of water-in-oil and oil-in-water emulsions even after the above-mentioned tests, offering us two types of promising membrane products with high selectivity and efficiency for water/oil separation. We believe this research will put forward a theoretical foundation to extend the practical applications for cotton fabric, showing its broad and important potential not only in filtration but also in the medical field.

Conflicts of interest

There are no conflicts to declare.

Acknowledgements

The research was supported by the State Key Laboratory of Bio-Fibers and Eco-Textiles (Qingdao University) (K2019-08), Key Laboratory of Bio-based Material Science & Technology (Northeast Forestry University, Ministry of Education) (SWZ-MS201910), Project of Jilin Province Science and Technology Development Research (20190103110JH, 20200301046RQ), National Natural Science Foundation of China (31971616, 31800480), Science and Technology Innovation Development Plan of Jilin City (20200104083) and Fundamental Research Funds for the Wood Material Science and Engineering Key Laboratory of Jilin Province.

Notes and references

1 M. A. Shannon, P. W. Bohn, M. Elimelech, J. G. Georgiadis, B. J. Mariñas and A. M. Mayes, Science and technology for water purification in the coming decades, *Nature*, 2008, **452**, 301–310.

2 A. K. Kota, G. Kwon, W. Choi, J. M. Mabry and A. Tuteja, Hygro-responsive membranes for effective oil-water separation, *Nat. Commun.*, 2012, **3**, 1025.

3 N. Liu, Y. Z. Cao, X. Lin, Y. N. Chen, L. Feng and Y. Wei, A facile solvent-manipulated mesh for reversible oil/water separation, *ACS Appl. Mater. Interfaces*, 2014, **6**, 12821–12826.

4 Z. J. Cheng, C. Li, H. Lai, Y. Du, H. W. Liu, M. Liu, K. N. Sun, L. G. Jin, N. Q. Zhang and L. Jiang, Recycled superwetting nanostructured copper mesh film: toward bidirectional separation of emulsified oil/water mixtures, *Adv. Mater. Interfaces*, 2016, **3**, 1600370.

5 W. B. Zhang, F. Liu, G. X. Liu, W. T. Gan, M. Zhang, H. Yu, X. Di, Y. Z. Wang and C. Y. Wang, Stimulus-responsive smart foam with dual wettability for transfer and controllable release of carbon tetrachloride, *Adv. Mater. Interfaces*, 2016, **3**, 1600100.

6 C. Schlaich, L. C. Camacho, L. X. Yu, K. Achazi, Q. Wei and R. Haag, Surface-independent hierarchical coatings with super-amphiphobic properties, *ACS Appl. Mater. Interfaces*, 2016, **8**, 29117–29127.

7 H. L. Che, M. Huo, L. Peng, T. Fang, N. Liu, L. Feng, Y. Wei and J. Y. Yuan, CO_2-responsive nanofibrous membranes with switchable oil/water wettability, *Angew. Chem.*, 2015, **127**, 9062–9066.

8 Z. Shami, S. M. Amininasa and P. Shakeri, Structure-property relationships of nanosheeted 3D hierarchical roughness MgAl-layered double hydroxide branched to an electrospun porous nanomembrane: a superior oil-removing nanofabric, *ACS Appl. Mater. Interfaces*, 2016, **8**, 28964–28973.

9 F. Xia and L. Jiang, Bio-inspired, smart: multiscale interfacial materials, *Adv. Mater.*, 2008, **20**, 2842–2858.

10 Y. Hong, E. Liu, J. Shi, X. Lin, L. Sheng, M. Zhang, L. Wang and J. Chen, A direct one-step synthesis of ultrathin g-C_3N_4 nanosheets from thiourea for boosting solar photocatalytic H_2 evolution, *Int. J. Hydrogen Energy*, 2019, **44**, 7194–7204.

11 J. Zimmermann, F. A. Reifler, G. Fortunato, L. C. Gerhardt and S. Seeger, A simple, one-step approach to durable and robust superhydrophobic fabrics, *Adv. Funct. Mater.*, 2008, **18**, 3662–3669.

12 B. Deng, R. Cai, Y. Yu, H. Q. Jiang, C. L. Wang, J. Li, L. F. Li, M. Yu, J. Y. Li, L. D. Xie, Q. Huang and C. H. Fan, Laundering Durability of Superhydrophobic Cotton Fabric, *Adv. Mater.*, 2010, **22**, 5473–5477.

13 R. Fürstner, W. Barthlott, C. Neinhuius and P. Walzel, Wetting and self-cleaning properties of artificial superhydrophobic surfaces, *Langmuir*, 2005, **21**, 956–961.

14 Z. J. Wei, W. L. Liu, D. Tian, C. L. Xiao and X. Q. Wang, Preparation of lotus-like superhydrophobic fluoropolymer films, *Appl. Surf. Sci.*, 2010, **256**, 3972–3976.

15 S. L. Wang, C. Y. Liu, G. C. Liu, M. Zhang, J. Li and C. Y. Wang, Fabrication of superhydrophobic wood surface by a sol-gel process, *Appl. Surf. Sci.*, 2011, **258**, 806–810.

16 Y. Gao, C. L. He and F. L. Qing, Polyhedral oligomeric silsesquioxane-based fluoroether-containing terpolymers: synthesis, characterization and their water and oil repellency evaluation for cotton fabric, *J. Polym. Sci., Part A: Polym. Chem.*, 2011, **49**, 5152–5161.

17 M. Zhang, S. L. Wang, J. Li and C. Y. Wang, A facile method to fabricate superhydrophobic cotton fabrics, *Appl. Surf. Sci.*, 2012, **261**, 561–566.

18 H. Zhou, H. X. Wang, H. T. Niu, A. Gestos, X. G. Wang and T. Lin, Fluoroalkyl silane modified silicone rubber/nanoparticle composite: a super durable, robust superhydrophobic fabric coating, *Adv. Mater.*, 2012, **24**, 2409–2412.

19 H. X. Wang, Y. H. Xue, J. Ding, L. F. Feng, X. G. Wang and T. Lin, Durable, self-healing superhydrophobic and superoleophobic surfaces from fluorinated-decyl polyhedral oligomeric silsesquioxane and hydrolyzed fluorinated alkyl silane, *Angew. Chem., Int. Ed.*, 2011, **123**, 11635–11638.

20 Z. J. Wang, Y. Wang and G. J. Liu, Rapid and efficient separation of oil from oil-in-water emulsions using a Janus cotton fabric, *Angew. Chem.*, 2016, **128**, 1313–1316.

21 H. C. Yang, J. W. Hou, V. Chen and Z. K. Xu, Janus membranes: exploring duality for advanced separation, *Angew. Chem., Int. Ed.*, 2016, **55**, 13398–13407.

22 S. Seyedin, J. M. Razal, P. C. Innis, A. Jeiranikhameneh, S. Beirne and G. G. Wallace, Knitted strain sensor textiles of highly conductive all-polymeric fibers, *ACS Appl. Mater. Interfaces*, 2015, **7**, 21150–21158.

23 Z. F. Wang, Y. Huang, J. F. Sun, Y. Huang, H. Hu, R. J. Jiang, W. M. Gai, G. M. Li and C. Y. Zhi, Polyurethane/cotton/carbon nanotubes core-spun yarn as high reliability stretchable strain sensor for human motion detection, *ACS Appl. Mater. Interfaces*, 2016, **8**, 24837–24843.

24 S. Rajeshkumar, C. Malarkodi, M. Vanaja and G. Annadura, Anticancer and enhanced antimicrobial activity of biosynthesizd silver nanoparticles against clinical pathogens, *J. Mol. Struct.*, 2016, **1116**, 165–173.

25 W. Jahn, Biological synthesis of silver nanoparticles using Svensonia hyderabadensis leaf extract and evaluation of their antimicrobial efficacy, *J. Struct. Biol.*, 1999, **127**, 106–112.

26 J. Y. Huang, S. H. Li, M. Z. Ge, L. N. Wang, T. L. Xing, G. Q. Chen, X. F. Liu, S. S. Al-Deyab, K. Q. Zhang, T. Chen and Y. K. Lai, Robust superhydrophobic TiO_2@fabrics for UV shielding, self-cleaning and oil-water separation, *J. Mater. Chem. A*, 2015, **3**, 2825–2832.

27 M. Zhang, J. Li, D. L. Zang, Y. Lu, Z. X. Gao, J. Y. Shi and C. Y. Wang, Preparation and characterization of cotton fabric with potential use in UV resistance and oil reclaim, *Carbohydr. Polym.*, 2016, **137**, 264–270.

28 M. M. Tao, L. X. Xue, F. Liu and L. Jiang, An intelligent superwetting PVDF membrane showing switchable transport performance for oil/water separation, *Adv. Mater.*, 2014, **26**, 2943–2948.

29 M. Yoshinari, Y. Oda, T. Kato, K. Okuda and A. Hirayama, Influence of surface modifications to titanium on oral bacterial adhesion in vitro, *Biomaterials*, 2001, **22**, 2043–2048.

